

## RESEARCH ARTICLE

# Extremely low-profile wideband array antenna using TCDA with polarization convertor

Seongjung Kim  | Sangwook Nam

The Institute of New Media Communication (INMC), School of Electrical and Computer Engineering, Seoul National University, Seoul, South Korea

## Correspondence

Sangwook Nam, The Institute of New Media Communication (INMC), School of Electrical and Computer Engineering, Seoul National University, Seoul 08826, South Korea.

Email: snam@snu.ac.kr

## Funding information

Bio-Mimetic Robot Research Center Funded by Defense Acquisition Program Administration, and by Agency for Defense Development, Grant/Award Number: UD190018ID

## Abstract

Herein, an extremely low-profile and wideband array antenna is proposed whose height is  $0.03 \lambda_{\text{low}}$  at the lowest operating frequency. The development of the proposed array antenna is described, and its performance is compared with those of conventional patch arrays, stacked patch arrays, planar ultrawideband modular antenna arrays, and tightly coupled dipole arrays (TCDAs). Furthermore, the impedance bandwidth is 98.2% at broadside radiation, and the overlapped bandwidth when scanning up to  $30^\circ$  is 95.9%. This high figure of merit is obtained by introducing a polarization convertor. Finally, the measured active VSWR and array gain of the fabricated  $6 \times 6$  array antenna are discussed. The measured result is in good agreement with the simulated result.

## KEYWORDS

compact antenna, extremely low-profile, phased array, polarization convertor, TCDA, wideband

## 1 | INTRODUCTION

To meet future demands and cover the desired frequency bands, the use of multiple sensors has been necessitated in

several RF communication systems. To implement such a multiple sensor-based antenna, the multifunctional array was proposed. It can reduce the number of antennas required and the cost of communication systems.<sup>1</sup> In addition, low-profile array antennas are indispensable for several wireless electronic systems. In this regard, TCDA antennas have attracted extensive attention owing to their several advantages, including the above-mentioned features.<sup>2–5</sup> As the phase of the wave reflected from the ground plane is reversed in such antennas, the impedance matching of an antenna that is close to the ground plane is difficult. However, the capacitance arising from the tight coupling between dipoles counteracts the reflected wave. Thus, TCDAs can be employed to fabricate low-profile and wideband antennas. Furthermore, the height of such array antennas has decreased to  $0.08 \lambda_{\text{low}}$  at the lowest operating frequency, and broadside radiation with an impedance bandwidth (IBW) of more than 150% has been achieved.<sup>6,7</sup> However, owing to the features of their vertical PCB structure, they cannot be favored for some applications. For planar and wideband array antennas, Vouvakis et al proposed the planar ultrawideband modular antenna arrays (PUMA).<sup>8</sup> Although the IBWs of PUMAs are in general narrower than those of TCDAs, they have a more stable configuration owing to their planar substrates and can be easily integrated to many platforms.

Furthermore, a microstrip patch antenna has several favorable characteristics, including an extremely low-profile, light weight, and ease of fabrication.<sup>9</sup> However, microstrip patch antennas have the shortcoming of a narrow bandwidth because of their resonant behavior. The bandwidth of planar antennas such as a microstrip patch antenna increases as the substrate becomes thicker, and decreases as the permittivity of the substrate becomes higher.<sup>10</sup> Therefore, a patch antenna with several substrate layers, including air gaps, was proposed to increase the bandwidth<sup>11</sup>; however, the size of this antenna was relatively large, and the design required 11 stacked-up layers. To simultaneously achieve both compactness and a low-profile with a wide bandwidth, several stacked patch antennas were proposed.<sup>10,12,13</sup>

Other efforts have also been made to obtain an extremely low-profile or low-profile antenna by replacing the ground plane of the antenna by an artificial magnetic conductor (AMC).<sup>14–19</sup> The use of an AMC enables the phase of the wave reflected from the ground plane to be in-phase. The bandwidth depends on the structure of AMCs. There are wideband AMC with proper shape.<sup>20,21</sup>

In this letter, to overcome the above-mentioned limitations, a planar extremely low-profile wideband TCDA with a polarization convertor (PC) is proposed herein. It is the first type of array antenna that has extremely low-profile and wideband characteristics simultaneously. The novel contribution of this work is that the wave reflected by the PC is rotated and changes its polarization so that it does not interact with the antenna, which makes the antenna extremely low-profile.

## 2 | DESIGN OF ANTENNA STRUCTURE AND OPERATION

The development of the proposed unit cell of the antenna is shown in Figure 1. All dielectric layers are FR-4 materials ( $\epsilon_r = 4.3$ ,  $\tan \delta = 0.025$ ), and the simulations were performed using the Computer Simulation Technology (CST) EM tool. First, the unit element of the TCDA with a  $200 \Omega$  discrete port and the dimensions on the four layers  $\alpha$ ,  $\beta$ ,  $\gamma$ ,

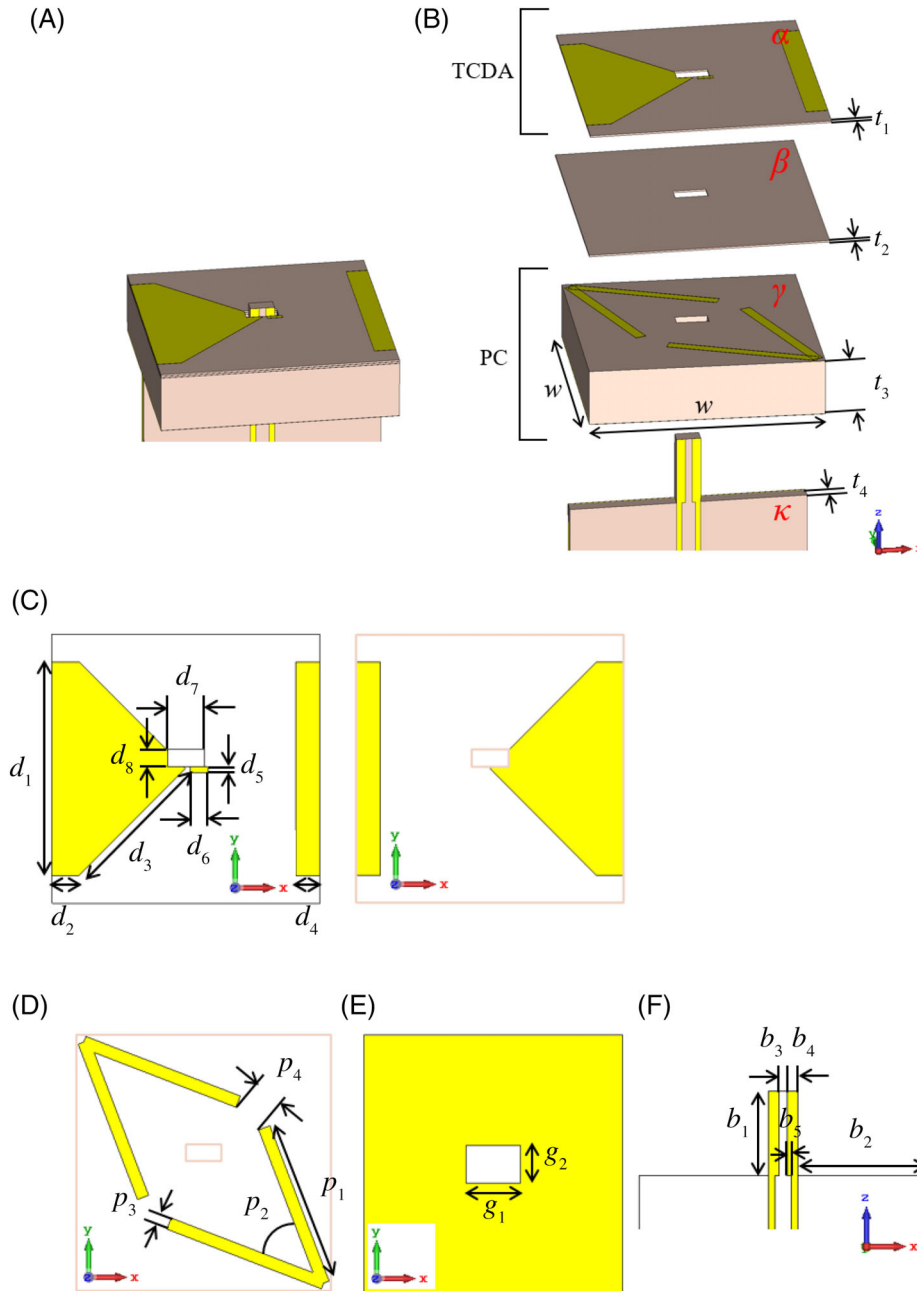


**FIGURE 1** Configuration of the proposed unit element. A, The proposed unit element. B, Exploded view of the unit element.  $w = 27.7$ ,  $t_1 = 0.2$ ,  $t_2 = 0.2$ ,  $t_3 = 6.6$ , and  $t_4 = 1.6$ . C, Top and bottom of layer  $\alpha$ . D, Top of layer  $\gamma$ . E, Ground plane (GP): bottom of layer  $\gamma$ . F, Top of layer  $\kappa$ .  $\beta$  layer is dummy for isolation between  $\alpha$  and  $\gamma$ .  $d_1 = 22$ ,  $d_2 = 2.8$ ,  $d_3 = 15.56$ ,  $d_4 = 2.5$ ,  $d_5 = 0.6$ ,  $d_6 = 1.8$ ,  $d_7 = 3.82$ ,  $d_8 = 1.8$ ,  $p_1 = 18$ ,  $p_2 = 48$ ,  $p_3 = 1.3$ ,  $p_4 = 3.47$ ,  $g_1 = 5.8$ ,  $g_2 = 4$ ,  $b_1 = 8.07$ ,  $b_2 = 12.44$ ,  $b_3 = 0.78$ ,  $b_4 = 1.02$ , and  $b_5 = 0.4$  (unit: mm) [Color figure can be viewed at [wileyonlinelibrary.com](http://wileyonlinelibrary.com)]

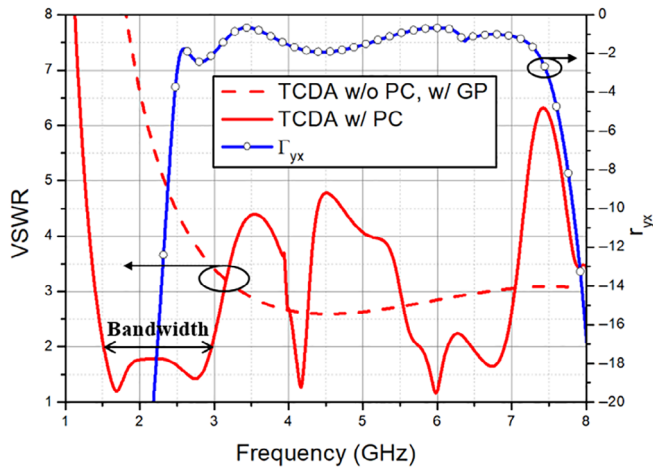


**FIGURE 2** Simulated VSWR of the unit cell with and without the PC, and polarization conversion ratio  $\Gamma_{yx}$  ( $=|E_{r,y}|/|E_{i,x}|$ ) of the PC unit cell (without the TCDA) at broadside direction where  $|E_{r,y}|$  is y-polarized reflected electric field from the PC and  $|E_{i,x}|$  is x-polarized incident electric field to the PC [Color figure can be viewed at [wileyonlinelibrary.com](http://wileyonlinelibrary.com)]

and  $\kappa$  are presented. The unit element of the PC is designed with the same dimension  $w$  as that of the unit element of the TCDA based on.<sup>22</sup> Since the electrical length of height is very small at 1.51-2.97 GHz (1.97:1), the reflected wave from the ground plane in the conventional TCDA is almost out of phase, and it is difficult to match the antenna impedance as shown in Figure 2 (dashed curve). However, if the PC is introduced under the TCDA, the polarization of the reflected wave is rotated 90° so that it has the orthogonal polarization with the dipole antenna. Since the dipole does not interact with the orthogonally polarized wave, the situation is equivalent to that there is no reflected wave to the dipole and the impedance matching can be achieved. The PC rotates the x-polarization to y-polarization and its operating band for  $\Gamma_{yx} > -2$  dB is approximately 2.98-7.35 GHz (2.47:1), which is not the band corresponding to 1.51-2.97 GHz (1.97:1). We found that the integration of TCDA and PC with very small gap  $t_2$ , the lowest operating frequency of the PC is shifted-down by half in this case. We

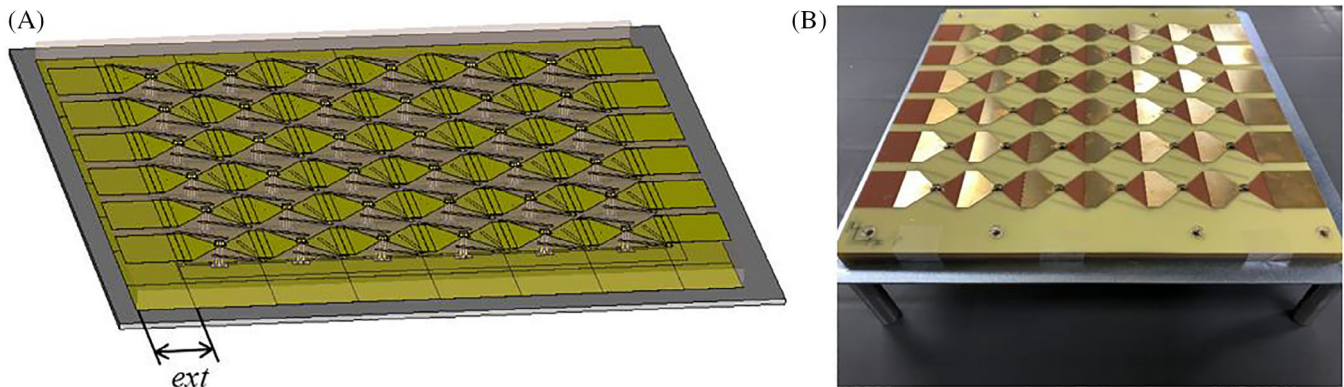


**FIGURE 3** Configuration of the  $6 \times 6$  proposed array antenna. A, Simulated configuration of the prototype array antenna. B, Photo of the fabricated antenna.  $Ext = 17.5$  mm [Color figure can be viewed at [wileyonlinelibrary.com](http://wileyonlinelibrary.com)]

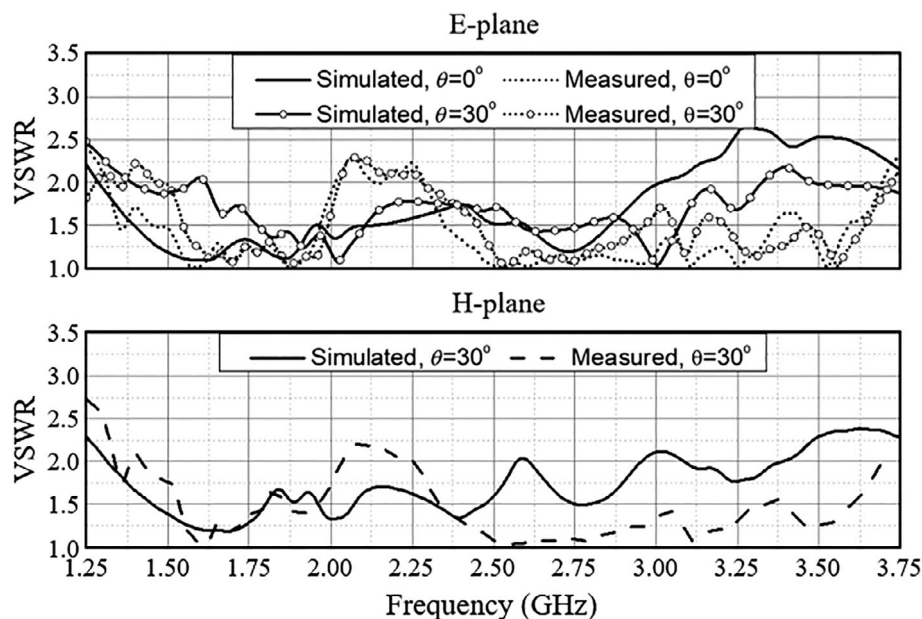


**FIGURE 4** Active VSWR at the center element (3, 3)

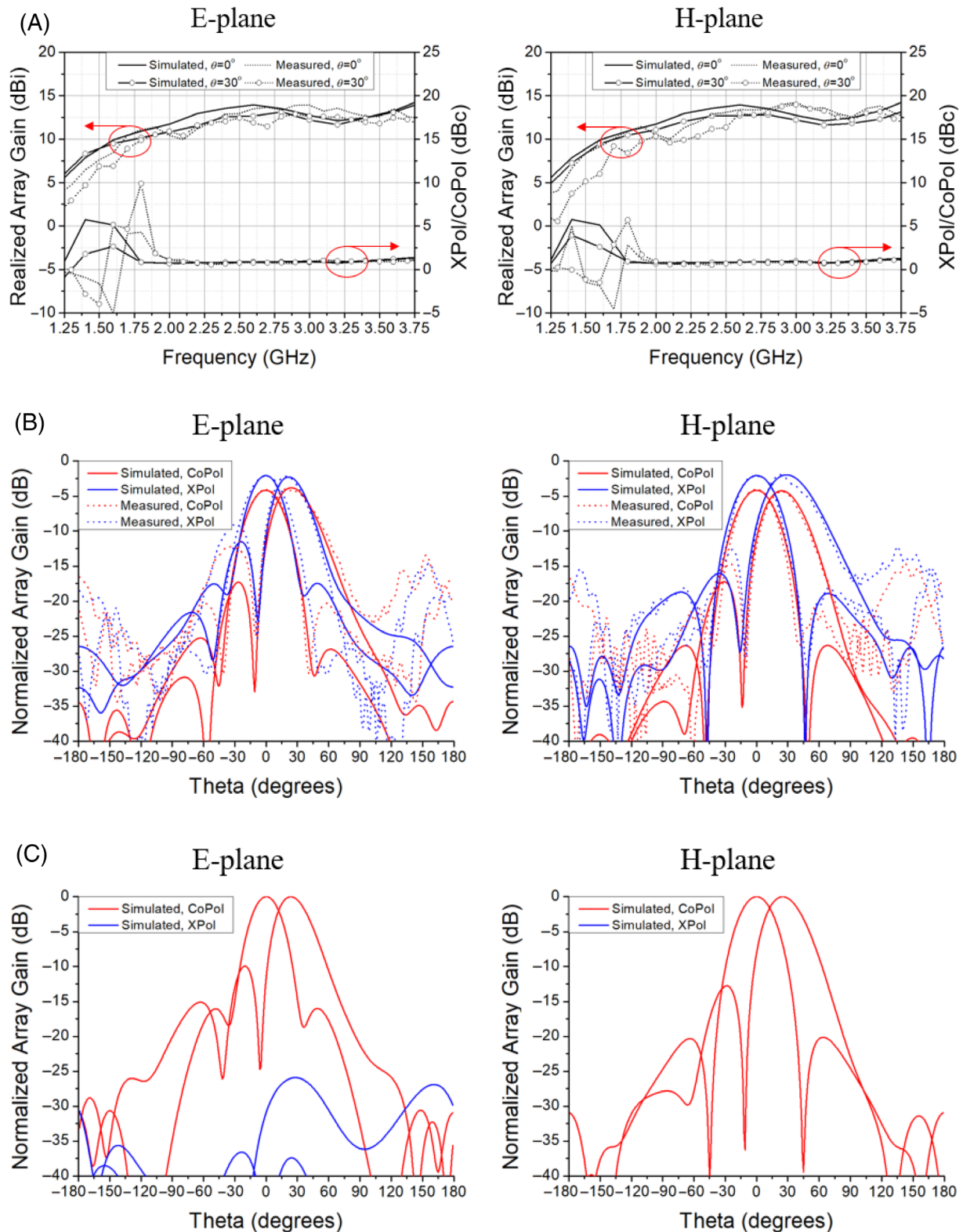


**FIGURE 5** A, Simulation and measurement results of realized array gain and XPoL/CoPo ratio. B, Normalized CoPol and XPoL gain patterns of the TCDA with and (C) without the PC at 2.5 GHz on the E-plane and H-plane when scanning the beam up to  $30^\circ$ . These are normalized by the absolute gain value [Color figure can be viewed at [wileyonlinelibrary.com](http://wileyonlinelibrary.com)]

guess near-field coupling due to very small gap between the PC and TCDA changes the operating band of the PC. Otherwise, for the case of large gap between them, the polarization is not rotated at the band (1.51–2.97 GHz).

It is necessary to introduce via holes into the multilayer substrates because the feeding lines should go through the ground plane. In addition, to achieve near-field coupling for large amount of energy between the PC and TCDA, the



**TABLE 1** Performance comparison of proposed and previous antennas

Type	Ref.	IBW (GHz, %)	Broadside gain (dBi)	Dimensions ( $\lambda_{\text{low}}^3$ )	Array size	Referenced VSWR
Patch	9	2.98-3.05, 2.32	Not given	$0.34 \times 1.16 \times 0.015$	$1 \times 3$	<2.25
Stacked patch	13	8.77-12.56, 35.4	16.5-20.9	$2.92 \times 2.92 \times 0.06$	$4 \times 4$	<2.07
AMC-based	20	1.67-2.98, 56.3	6.8-7.5	$0.84 \times 1.06 \times 0.1$	$1 \times 1$	<2.25
	21	1.65-1.88, 13	12.2-12.8	$3.08 \times 0.55 \times 0.1$	$1 \times 4$	<2.25
		1.89-2.22, 16.1	12.3-13.2	$3.53 \times 0.63 \times 0.11$	$1 \times 4$	
PUMA	8	3.28-20, 143.6	Not given	$1.32 \times 1.32 \times 0.07$	$16 \times 16$	<2.87
TCDA	6	0.6-4.68, 154	4.1-20	$0.45 \times 0.69 \times 0.08$	$8 \times 8$	<2.25
	7	0.3-2.21, 151.9	0.2-19.9	$0.39 \times 0.39 \times 0.08$	$8 \times 8$	<2.25
PC-based	This Work	1.28-3.75, 98.2	4.71-12.34	$0.97 \times 0.97 \times 0.03$	$6 \times 6$	<2.25

distance between them should be very small: 0.2 mm ( $=h_1 - h_2$ ) in this case. However, there are many limitations with regard to fabrication of via holes through multilayer with various thicknesses that we had designed. Thus, in this letter, we utilized alternative to via holes. This method is very simple and free of limitations such as the unfavorable thicknesses and permittivity of the layers. As shown in Figure 1B, the vertical substrate under the ground plane is inserted from the ground plane to the top of structure. The coplanar strip lines acts as via holes. Under the ground plane, the wideband balun chip, which transforms 200  $\Omega$  to 50  $\Omega$  (bandwidth: 20-4500 MHz, TCM4-452X+, <https://www.minicircuits.com>) is mounting on the vertical layer.

### 3 | SIMULATED AND EXPERIMENTAL RESULTS FOR THE PROPOSED $6 \times 6$ ARRAY ANTENNA

Figure 3 shows the proposed  $6 \times 6$  finite array antenna. The edge arms of the array in the E-plane are extended by *ext* to improve the impedance matching of the edge elements and dimensions of the full structure are  $226.2 \times 226.2 \times 7$  mm<sup>3</sup>. The array antenna is supported by a steel ground plane. Measurement is performed by the method described in,<sup>23</sup> which is the summation of the weighted S-parameters. The active VSWR of the proposed array is simulated and measured at the center element (3, 3) and shown in Figure 4. The simulated IBW for VSWR <2.25 is 1.25-3.16 GHz (86.6%) when scanning to the broadside direction, and the measured IBW is 1.28-3.75 GHz (98.2%). The height of the array antenna ( $=t_1 + t_2 + t_3$ ) is  $0.03 \lambda_{\text{low}}$  at the lowest operating frequency, 1.28 GHz. The measured overlapped IBW when scanning up to 30° is 1.32-3.75 GHz (95.9%). The gain patterns are measured in an anechoic chamber and postprocessed following the procedure.<sup>24</sup> Figure 5A shows the simulation and measurement results of the proposed CoPol and XPol array gains, and XPol/CoPol ratio, as the beam is scanned up to 30° on the E- and H-planes. The principle direction of co-

polarization is *x*-direction at broadside and the cross-polarization is orthogonal to it. The simulated peak array gain is 13.9 dBi in the E and H-planes. The measured peak array gain is 14.3 dBi in all planes, and it is in good agreement with the simulated results. Figure 5B,C shows the simulated and measured normalized gain patterns of the TCDA with and without the PC at 2.5 GHz, as the main beam is scanned up to 30°, respectively. It is observed that the cross-polarization level of the TCDA with the PC is comparable with the co-polarization level although the co-polarization beam shapes of two cases are same. The measured results are in good agreement with the simulated results of the main beam.

Finally, the proposed array antenna is compared with conventional patch arrays, stacked patch arrays, arrays based on AMCs, PUMA arrays, and TCDAs as shown in Table 1. The reference used for comparison is the IBW when scanning to broadside direction. The height of the array antenna refers to the electrical distance between the ground plane and the highest plane of the antenna structure at the lowest operating frequency. The AMC-based antenna<sup>21</sup> has dual bandwidth. As can be seen the Table 1, the IBW of the proposed array antenna is wider than those of conventional patch arrays, stacked patch arrays, and arrays based on AMCs. Furthermore, the height is lower than any of them except for conventional patch arrays. In contrast, the IBW of the proposed antenna is narrower than those of PUMA arrays and TCDAs. However, the height of the proposed array antenna is much lower. Considering the figure of merit, Table 1 shows that the proposed array antenna has a high figure of merit, which means it is an extremely low-profile and wideband array antenna.

### 4 | CONCLUSION

In this letter, we show that an array antenna with very wide IBW of 98.2% can be designed with a height of  $0.03 \lambda_{\text{low}}$  which is comparable to that of a conventional patch array

antenna. This is enabled by TCDA employing the closely positioned PC. The measured peak array gain is 14.3 dBi in all planes, and the same beam width and radiated directions are obtained. It can be used for applications that require a high absolute array gain without polarization purity.

## ACKNOWLEDGMENTS

This research was supported by a grant to Bio-Mimetic Robot Research Center Funded by Defense Acquisition Program Administration, and by Agency for Defense Development (UD190018ID).

## ORCID

Seongjung Kim  <https://orcid.org/0000-0001-5189-8023>

## REFERENCES

- [1] Tavik GC, Hilterbrick CL, Evins JB, et al. The advanced multifunction RF concept. *IEEE Trans Microw Theory Tech*. 2005;53(3):1009-1020.
- [2] Volakis JL, Sertel K. Narrowband and wideband metamaterial antennas based on degenerate band edge and magnetic photonic crystals. *Proc IEEE*. 2011;99(10):1732-1745.
- [3] Yetisir E, Ghalichechian N, Volakis JL. Ultrawideband array with 70° scanning using FSS superstrate. *IEEE Trans Antennas Propag*. 2016;64(10):4256-4265.
- [4] Wenyang Z, Chen Y, Yang S. Dual-polarized tightly coupled dipole array for UHF–X-band satellite applications. *IEEE Antennas Wirel Propag Lett*. 2019;18(3):467-471.
- [5] Novak MH, Miranda FA, Volakis JL. Ultra-wideband phased array for small satellite communications. *IET Microw Antennas Propag*. 2017;11(9):1234-1240.
- [6] Doane JP, Sertel K, Volakis JL. A wideband, wide scanning tightly coupled dipole array with integrated balun (TCDA-IB). *IEEE Trans Antennas Propag*. 2013;61(9):4538-4548.
- [7] Zhang H, Yang S, Xiao SW, Chen Y, Qu SW, Hu J. Ultrawideband phased antenna arrays based on tightly coupled open folded dipoles. *IEEE Antennas Wirel Propag Lett*. 2019;18(2):378-382.
- [8] Logan JT, Kindt RW, Lee MY, Vouvakis MN. A new class of planar ultrawideband modular antenna arrays with improved bandwidth. *IEEE Trans Antennas Propag*. 2017;66(2):692-701.
- [9] Yusuf Y, Gong X. A low-cost patch antenna phased array with analog beam steering using mutual coupling and reactive loading. *IEEE Antennas Wirel Propag Lett*. 2008;7:81-84.
- [10] Lee HJ, Li ES, Jin H, Li CY, Chin KS. 60 GHz wideband LTCC microstrip patch antenna array with parasitic surrounding stacked patches. *IET Microw Antennas Propag*. 2018;13(1):35-41.
- [11] Serra AA, Nepa P, Manara G, Tribellini G, Cioci S. A wide-band dual-polarized stacked patch antenna. *IEEE Antennas Wirel Propag Lett*. 2007;6:141-143.
- [12] Xu J, Hong W, Jiang ZH, Zhang H. Wideband, low-profile patch array antenna with corporate stacked microstrip and substrate integrated waveguide feeding structure. *IEEE Trans Antennas Propag*. 2018;67(2):1368-1373.
- [13] Bilgic MM, Yegin K. Wideband offset slot-coupled patch antenna array for X/Ku-band multimode radars. *IEEE Antennas Wirel Propag Lett*. 2014;13:157-160.
- [14] Yan S, Ping JS, Vandenbosch GAE. Low-profile dual-band textile antenna with artificial magnetic conductor plane. *IEEE Trans Antennas Propag*. 2014;62(12):6487-6490.
- [15] Cook BS, Shamim A. Utilizing wideband AMC structures for high-gain inkjet-printed antennas on lossy paper substrate. *IEEE Antennas Wirel Propag Lett*. 2013;12:76-79.
- [16] Zhai H, Xi L, Zang Y, Li L. A low-profile dual-polarized high-isolation MIMO antenna arrays for wideband base-station applications. *IEEE Trans Antennas Propag*. 2017;66(1):191-202.
- [17] Li M, Li Q, Wang B, Zhou C, Cheung S. A miniaturized dual-band base station array antenna using band notch dipole antenna elements and AMC reflectors. *IEEE Trans Antennas Propag*. 2018;66(6):3189-3194.
- [18] Yang W, Wang H, Che W, Wang J. A wideband and high-gain edge-fed patch antenna and array using artificial magnetic conductor structures. *IEEE Antennas Wirel Propag Lett*. 2013;12:769-772.
- [19] Lin W, Chen SL, Ziolkowski RW, Guo YJ. Reconfigurable, wideband, low-profile, circularly polarized antenna and array enabled by an artificial magnetic conductor ground. *IEEE Trans Antennas Propag*. 2018;66(3):1564-1569.
- [20] Li M, Li QL, Wang B, Zhou CF, Cheung SW. A low-profile dual-polarized dipole antenna using wideband AMC reflector. *IEEE Trans Antennas Propag*. 2018;66(5):2610-2615.
- [21] Li M et al. A miniaturized dual-band dual-polarized band-notched slot antenna array with high isolation for base station applications. *IEEE Trans Antennas Propag*. 2019;68(2):795-804.
- [22] Gao X, Han X, Cao WP, Li HO, Ma HF, Cui TJ. Ultrawideband and high-efficiency linear polarization converter based on double V-shaped metasurface. *IEEE Trans Antennas Propag*. 2015;63(8):3522-3530.
- [23] Vouvakis MN, Schaubert DH. Vivaldi antenna arrays. *Frontiers in Antennas: Next Generation Design Engineering*. New York, NY: McGraw-Hill; 2011.
- [24] Kelley DF, Stutzman WL. Array antenna pattern modeling methods that include mutual coupling effects. *IEEE Trans Antennas Propag*. 1993;41(12):1625-1632.

**How to cite this article:** Kim S, Nam S. Extremely low-profile wideband array antenna using TCDA with polarization convertor. *Microw Opt Technol Lett*. 2021;63:959–964. <https://doi.org/10.1002/mop.32694>